PERGAMON

International Journal of Heat and Mass Transfer 43 (2000) 2221–2231

International Journal of HEAT and MASS TRANSFER

www.elsevier.com/locate/ijhmt

The well-posedness of incompressible one-dimensional two-fluid model

Jin Ho Song [a,*], M. Ishii [b]

[a] Korea Atomic Energy Research Institute, PO Box 105, Yusong Post Office, Taejon 305-600, South Korea
[b] School of Nuclear Engineering, 1290 Nuclear Engineering Building, Purdue University, West Lafayette, IN 47907-1290, USA

Received 16 October 1998

Abstract

A characteristic analysis on the stability of the governing differential equations for an incompressible one-dimensional two-fluid model is presented. The stability criteria are newly proposed in terms of the momentum flux parameters by incorporating the effect of void fraction and velocity profiles. A simplified two-phase flow configuration constructed by using existing correlation for distribution parameter and experimentally correlated velocity profiles is selected to test the validity of the proposed theory. The curve of calculated momentum flux parameters is compared with the curve of stability criteria. The simplified flow is found to be stable within a wide range of void fraction.

1. Introduction

As the two-phase flow in a pipe or channel can be described by an area averaged one-dimensional two-fluid model [1,2], the one-dimensional two-fluid model is widely employed in many computer codes, such as RELAP5/MOD3 [3]. Recently, there were studies on the well-posedness of the one-dimensional two fluid model. They investigated the validity of governing differential equations and constitutive relations by performing characteristic analyses on the stability of differential equations [4–11]. They indicated that the governing differential equations of the one-dimensional two-fluid model could be ill-posed as an initial value problem. The inclusion of the virtual mass force term and viscous term resulted in some improvement of the stability of the differential equation [3,7]. However, as the correct forms of those terms are yet unknown and those terms have a transient effect, the well-posedness is still an open issue. Here, we revisited the issue of well-posedness of the two-fluid model equations. The role of momentum flux parameters, which accounts for the effect of void fraction and velocity profile changes over a flow area, is investigated in terms of the well-posedness of governing differential equations.

2. One-dimensional two-fluid model

The area averaged one-dimensional two-fluid model is very useful for complicated engineering problems. The one-dimensional two-fluid model can be obtained by integrating the three-dimensional two-fluid model over a cross-section and introducing proper mean values [1,2]. A simple area average over a cross-section is defined by

* Corresponding author. Tel.: +82-42-868-2850; fax: +82-42-861-2574.
E-mail address: dosa@nanum.kaeri.re.kr (J.H. Song).

0017-9310/00/$ - see front matter
PII: S0017-9310(99)00287-2

Nomenclature

B_d	volume of bubbles
C_D	drag coefficient
C_M	virtual mass coefficient
C_{vk}	momentum flux parameter of kth phase
D_b	bubble diameter
$D_g/D\xi$	material derivative with respect to gas velocity
D_d/D_t	material derivative with respect to dispersed phase velocity
F_D	drag force
F_V	virtual mass force
g	gravity vector
$\mathbf{M}_{ik}$	generalized drag force vector for kth phase
p_k	pressure of the kth phase
p_{ki}	interfacial pressure of the kth phase
r_b	bubble radius
r	non-dimensional radial position
t	time
u_k	velocity of the kth phase
v_c	velocity vector for continuous phase
$\mathbf{v}_k$	velocity vector of the kth phase
$\mathbf{v}_{ki}$	interfacial velocity of the kth phase
z	axial direction along pipe

Greek symbols

Γ_k	mass generation of the kth phase
α_k	void fraction of the kth phase
α	void fraction of gas
α_o	void fraction at center
α_w	void fraction at the wall
μ_m	mixture viscosity
θ	inclination angle of pipe from the vertical direction
ρ_c	density of continuous phase
ρ_k	density of the kth phase
τ_i	interfacial shear stress
τ_k	laminar shear stress of the kth phase
τ_k^t	turbulent shear stress of the kth phase
τ_{kw}	wall shear stress

Subcripts

f, g, k	liquid, gas, kth phase

$$\langle F\rangle = 1/A\int F\,\mathrm{d}A \tag{1}$$

and the void fraction weighted mean value is given by

$$\langle\langle F_k\rangle\rangle = \langle\alpha_k F_k\rangle/\langle\alpha_k\rangle \tag{2}$$

The density of each phase is considered to be uniform such that $\rho_k = \langle\rho_k\rangle$. The axial component of the weighted mean velocity of phase k is

$$\langle\langle u_k\rangle\rangle = \langle\alpha_k u_k\rangle/\langle\alpha_k\rangle \tag{3}$$

Then, the one-dimensional area averaged continuity equation is written as follows

$$\partial(\langle\alpha_k\rangle\rho_k)/\partial t + \partial(\langle\alpha_k\rangle\rho_k\langle\langle u_k\rangle\rangle)/\partial z = \langle\Gamma_k\rangle \tag{4}$$

Drop $\langle\rangle$, $\langle\langle\rangle\rangle$ notations for simplicity. Then, the continuity equation is written as

$$\alpha_k D\rho_k/Dt + \alpha_k\rho_k\partial u_k/\partial z + \rho_k\partial\alpha_k/\partial t + \rho_k u_k\partial\alpha_k/\partial z = \Gamma_k \tag{5}$$

where D/Dt is a material derivative. When we consider a simple adiabatic flow in a pipe or duct, we can assume incompressibility of gas and liquid phase. Then Eq. (5) can be written for gas and liquid phase as follows

$$\partial\alpha/\partial t + u_g\partial\alpha/\partial z + \alpha\partial u_g/\partial z = 0 \tag{6}$$

$$-\partial\alpha/\partial t - u_f\partial\alpha/\partial z + (1-\alpha)\partial u_f/\partial z = 0 \tag{7}$$

where α is gas void fraction.

The one-dimensional area averaged momentum equation is written as

$$\begin{aligned}&\partial\langle\alpha_k\rangle\rho_k\langle\langle u_k\rangle\rangle/\partial t + \partial(\langle\alpha_k\rangle\rho_k C_{vk}\langle\langle u_k\rangle\rangle^2)/\partial z\\ &= -\langle\alpha_k\rangle\partial p_k/\partial z - 4\alpha_{kw}\tau_{kw}/D\\ &+ \partial(\langle\alpha_k\rangle\langle\langle\tau_{kzz} + \tau^T_{kzz}\rangle\rangle)/\partial z + \langle\alpha_k\rangle\rho_k g\cos\theta\\ &+ (p_{ki} - p_k)\partial\alpha_k/\partial z + \langle\langle v_{ki}\rangle\rangle\langle\Gamma_k\rangle + \langle\mathbf{M}_{ik}\rangle_z\end{aligned} \tag{8}$$

For the adiabatic air–water flow $\Gamma_k = 0$. The area-averaged form of shear stress becomes $4\alpha_{kw}\tau_{kw}/D$. D is the hydraulic diameter of the pipe. C_{vk} is momentum flux parameter defined as

$$C_{vk} = \langle\alpha_k u_k^2\rangle/\langle\alpha_k\rangle\langle\langle u_k\rangle\rangle^2 \tag{9}$$

It accounts for the variation of velocity and void fraction over a cross-section. Therefore, it contains information on the flow structure. To investigate the stability of the differential equations we need to know the constitutive relations for various terms in the right hand side. The generalized drag force [2] can be represented as

$$M_{ig} = -M_{if} = \alpha F_D/B_d + \alpha F_v/B_d + 9/2\alpha/r_b\sqrt{(\rho_f\mu_m/\pi)}\int_t D_g/D\xi(u_f - u_g)d\xi/\sqrt{(t-\xi)} \quad (10)$$

where the standard drag force acting on the particle under steady-state conditions can be presented in terms of the drag coefficient C_D and relative velocity and the virtual mass term is represented as

$$\alpha F_v/B_d = C_M\rho_c(D_d v_r/Dt - v_r\nabla v_c) = C_M\rho_f[\partial(u_g-u_f)/\partial t + u_g\partial(u_g-u_f)/\partial z - (u_g-u_f)\partial u_f/\partial z)] \quad (11)$$

Previous studies [5–7,9] focused on the role of these forces on the stability of governing differential equations. It is found that the generalized force tends to stabilize the flow. Here, we want to focus on the role of momentum flux parameter by neglecting the contributions from virtual mass.

Let the algebraic terms of the right-hand side including generalized force be represented as $\mathbf{M}^*_{ik}$ and drop $\langle\rangle$, $\langle\langle\rangle\rangle$ notations for convenience. Then the momentum equations for the one-dimensional two-fluid model can be presented as follows

$$\rho_k u_k\partial\alpha_k/\partial t + \rho_k C_{vk}u_k^2\partial\alpha_k/\partial z + \alpha_k\rho_k\partial u_k/\partial t + \alpha_k\rho_k C_{vk}\partial u_k^2/\partial z + \alpha_k u_k D\rho_k/Dt + \alpha_k u_k^2(C_{vk}-1)\partial\rho_k/\partial z + \alpha_k\rho_k u_k^2\partial C_{vk}/\partial z = -\alpha_k\partial p_k/\partial z + \mathbf{M}^*_{ik} \quad (12)$$

C_{vk} is expected to be a function of velocities, densities, and void fraction. Here, we make an assumption that the momentum flux parameters represent a certain flow structure and are determined by the inlet flow conditions and flow geometry only. Then, it can be assumed that C_{vk} is invariant with flow direction, if the pipe or duct geometry is not changed. Then the above equation can be approximated by the following equation by assuming incompressibility of gas and liquid phase.

$$\rho_k u_k\partial\alpha_k/\partial t + \rho_k C_{vk}u_k^2\partial\alpha_k/\partial z + \alpha_k\rho_k\partial u_k/\partial t + \alpha_k\rho_k C_{vk}\partial u_k^2/\partial z = -\alpha_k\partial p_k/\partial z + \mathbf{M}^*_{ik} \quad (13)$$

By doing this, we might have lost mathematical rigorousness. However, Eq. (13) is a good first order approximation. Also by assuming that gas and liquid phase are at the same pressure, the gas and liquid momentum equations are written as

$$\alpha\rho_g\partial u_g/\partial t + \rho_g u_g\partial\alpha/\partial t + \rho_g C_{vg}u_g u_g\partial\alpha/\partial z + 2\alpha\rho_g C_{vg}u_g\partial u_g/\partial z = -\alpha\partial p/\partial z + M^*_{ig} \quad (14)$$

$$(1-\alpha)\rho_f\partial u_f/\partial_t - \rho_f u_f\partial\alpha/\partial t - \rho_f C_{vf}u_f u_f\partial\alpha/\partial z + 2(1-\alpha)\rho_f C_{vf}u_f\partial u_f/\partial z = -(1-\alpha)\partial p/\partial z + M^*_{if} \quad (15)$$

3. Change of type of the governing differential equations

3.1. Characteristic analysis

Let $\mathbf{x}$ be a vector $\mathbf{x}=(\alpha, u_g, u_f, p)$, then the system of continuity and momentum equations can be written as

$$[A]\partial\mathbf{x}/\partial t + [B]\partial\mathbf{x}/\partial z = [C] \quad (16)$$

where $[A]$, $[B]$, $[C]$ are the coefficient matrices. To investigate the behavior of this set of differential equations, suppose that arbitrary data for $\mathbf{x}$ are specified along a curve in z, t plane. Introduce the tangential variable $s(z, t)$ and normal variable $n(z, t)$ along the curve, then the above equation can be transformed as

$$\{[A]\partial n/\partial t + [B]\partial/\partial z\}\partial\mathbf{x}/\partial n = [C] - \{[A]\partial s/\partial t + [B]\partial s/\partial z\}\partial\mathbf{x}/\partial s \quad (17)$$

Since $\mathbf{x}$ is given by the initial data as a function of s along the curve, the terms on the right-hand side are known. Then the derivative $\partial\mathbf{x}/\partial n$ will be uniquely determined, if the determinant of the coefficient matrix is non-singular.

$$|\,[A]\partial n/\partial t + [B]\partial n/\partial z\,| \neq 0 \quad (18)$$

Therefore, the dependence of the solution on the prescribed initial data can be reduced to an investigation of the roots of equation

$$\text{Determinant of } \{[A]\lambda - [B]\} = f(\lambda) = 0 \quad (19)$$

where we have introduced the characteristic curve $\lambda = -\partial n/\partial t/\partial n/\partial z$.

If we have real roots of λ for satisfying $f(\lambda)=0$, then the set of differential equations is hyperbolic. If we have a complex conjugate root of λ, then the set of

differential equations becomes elliptic. In this case, the set of equations becomes ill-posed as an initial value problem. By using Eqs. (6), (7), (14), and (15), $[A]\lambda-[B]$ are determined as

$$\begin{vmatrix} \lambda-u_g & -\alpha & 0 & 0 \\ -(\lambda-u_f) & 0 & -(1-\alpha) & 0 \\ \rho_g u_g(\lambda-C_{vg}u_g) & \alpha\rho_g(\lambda-2C_{vg}u_g) & 0 & -\alpha \\ -\rho_f u_f(\lambda-C_{vf}u_f) & 0 & (1-\alpha)\rho_f(\lambda-2C_{vf}u_f) & 0 \end{vmatrix} \quad (20)$$

The determinant of this matrix becomes

$$f(\lambda) = -\alpha(1-\alpha)[(1-\alpha)\rho_g(\lambda\lambda - 2\lambda C_{vg}u_g + C_{vg}u_g u_g) + \alpha\rho_f(\lambda\lambda - 2C_{vf}u_f\lambda + C_{vf}u_f u_f)] \quad (21)$$

If we do not consider the effect of void distribution and velocity distribution across the pipe, the momentum flux distribution parameters are equal to 1. Then Eq. (21) becomes,

$$f(\lambda) = -\alpha(1-\alpha)[(1-\alpha)\rho_g(\lambda-u_g)^2 + \alpha\rho_f(\lambda-u_f)^2] \quad (22)$$

The equation $f(\lambda)=0$ can have real roots only if $\lambda=u_g=u_f$. It requires that gas and liquid speed should be equal. Otherwise, the two-fluid model becomes ill-posed as pointed out by Gidaspow [4]. For single-phase flow where α equals 1 or 0, Eq. (21) becomes

$$f(\lambda) = \rho_g(\lambda\lambda - 2\lambda C_{vg}u_g + C_{vg}u_g u_g), \text{ or } \rho_f(\lambda\lambda - 2C_{vf}u_f\lambda + C_{vf}u_f u_f) \quad (23)$$

It always has real characteristics, $\lambda=\sqrt{C_{vg}}u_g$, or $\lambda=\sqrt{C_{vf}}u_f$. Then, the governing differential equations are always hyperbolic type and well-posed.

Let us consider the effect of momentum flux distribution parameters. To have real roots for λ for the equation $f(\lambda)=0$, it is required from Eq. (21) that

$$F(\alpha, C_{vg}, C_{vf}, u_g, u_f, \rho_f, \rho_g) = [(1-\alpha)\rho_g C_{vg}u_g + \alpha\rho_f C_{vf}u_f][(1-\alpha)\rho_g C_{vg}u_g + \alpha\rho_f C_{vf}u_f] - [(1-\alpha)\rho_g + \alpha\rho_f][(1-\alpha)\rho_g C_{vg}u_g u_g + \alpha\rho_f C_{vf}u_f u_f] \geq 0 \quad (24)$$

Eq. (24) indicates that the momentum flux distribution parameters can make the two-fluid model have real roots without imposing the unrealistic condition that the liquid and gas velocity should be equal. It indicates that the void fraction and velocity distributions have a stabilizing effect. If we have positive $F(\alpha)$, the two-fluid model equation allows two real characteristic roots for λ. Since we assumed incompressible gas and liquid phase, the characteristic roots related to the sound speed do not appear here. It is clear that if momentum flux parameters behave in such a way that above inequality is always met, then the two-fluid model becomes well-posed.

3.2. Relation between C_{vg} and C_{vf}

Eq. (24) indicates that either C_{vg}, or C_{vf} need to be bigger than 1 to have real roots for $f(\lambda)=0$. Let $\rho_m=(1-\alpha)\rho_g+\alpha\rho_f$, $M_g=(1-\alpha)\rho_g C_{vg}u_g$, $M_f=\alpha\rho_f C_{vf}u_f$, then Eq. (24) can be rearranged as

$$\begin{aligned} &F(\alpha, C_{vg}, C_{vf}, u_g, u_f, \rho_f, \rho_g) \\ &= (M_g+M_f)^2 - \rho_m M_g u_g - \rho_m M_f u_f \\ &= (M_g + M_f - \rho_m u_g/2)^2 - \rho_m M_f u_f + \rho_m M_f u_g \\ &\quad - (\rho_m u_g/2)^2 \geq 0 \end{aligned} \quad (25)$$

It requires that

$$(M_g + M_f - \rho_m u_g/2)^2 \geq (\rho_m u_g/2)^2 - \rho_m M_f(u_g - u_f) \quad (26)$$

If the right-hand side of Eq. (26) is negative, above inequality is always met. Therefore, if the following inequality is met, the flow is stable.

$$4M_f(u_g-u_f) \geq \rho_m u_g^2 \quad (27)$$

Let $S=u_g/u_f$ and call it slip ratio and $R=\alpha\rho_f/((1-\alpha)\rho_g)$ and call it modified density ratio. Assume that u_f is positive. Then, if S is less than 1, above inequality requires C_{vf} be negative. It is not physically reasonable. If S is bigger than 1, it is required

$$C_{vf} \geq \tfrac{1}{4}[1/R+1]S^2/(S-1), \quad S>1 \quad (28)$$

When the right-hand side of Eq. (26) is positive, inequality (26) is equivalent to

$$M_g \geq 0.5\rho_m u_g + [(\rho_m u_g/2)^2 - \rho_m M_f(u_g-u_f)]^{1/2} - M_f \quad (29)$$

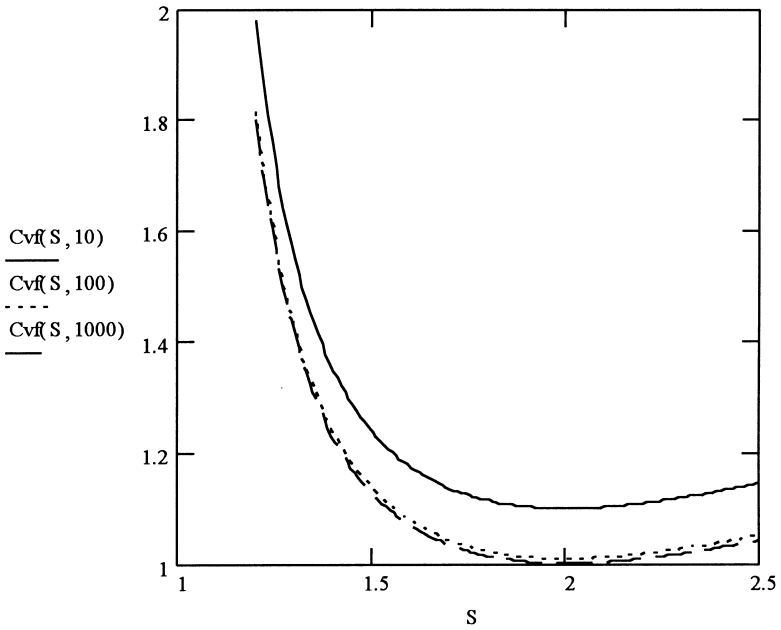

Fig. 1. Stability boundary presented by the liquid momentum flux parameter C_{vf} and the slip ratio S.

$$M_g \le 0.5\rho_m u_g - [(\rho_m u_g/2)^2 - \rho_m M_f(u_g - u_f)]^{1/2} - M_f \quad (30)$$

Let u_g be positive for convenience, then

$$C_{vg} \ge 0.5(1+R) + 0.5[(1+R)^2 - 4(1+R)RC_{vf}1/S^2(S-1)]^{1/2} - RC_{vf}1/S \quad (31)$$

$$C_{vg} \le 0.5(1+R) - 0.5[(1+R)^2 - 4(1+R)RC_{vf}1/S^2(S-1)]^{1/2} - RC_{vf}1/S \quad (32)$$

Eqs. (28), (31), and (32) define the stability boundary between the stable region and unstable region. Slip ratio S and modified density ratio R determine the boundary. When $S > 1$, two-fluid model can be stable if C_{vf} satisfies Eq. (28). If C_{vf} is less than that specified by Eq. (28), then C_{vg} and C_{vf} should satisfy Eq. (31) or (32). When $S \le 1$, the C_{vg} and C_{vf} should satisfy Eq. (31) or (32). Let us consider the case with $S > 1$, this is practical for vertical air–water flow. Then Eq. (28) indicates that if the liquid momentum flux parameter is bigger than a certain value, the flow is stable.

Fig. 1 shows the stability boundary in terms of liquid momentum flux parameter for various values of R at 1, 10, and 100 depending on the slip ratio S. Above the curve is the stable region. Fig. 2 shows boundaries of Eqs. (31) and (32) at $R = 100$ and $S = 2$. Above the upper curve and below the lower curve are stable regions. The upper curve represents Eq. (31) and lower curve represents Eq. (32). The upper curve is concave and encloses the square defined by (0, 0), (0, 1), (1, 0), (1, 1). In a real physical system C_{vg} and C_{vf} are close to 1. The lower curve does not seem to have physical meaning. The upper curve indicates that C_{vg} can be close to one only when C_{vf} is

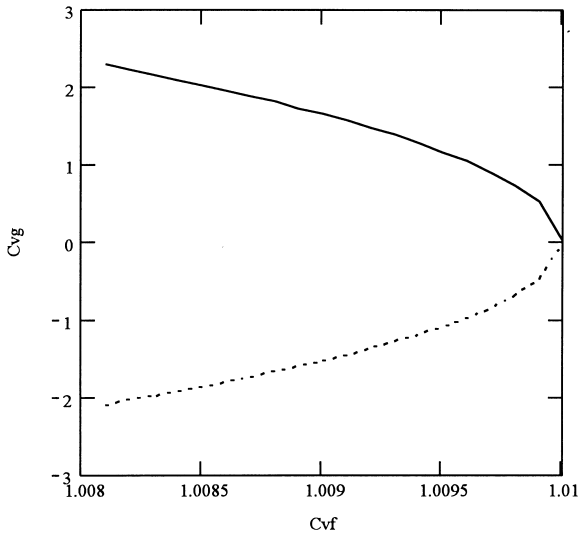

Fig. 2. Stability boundary presented by the gas momentum flux parameter C_{vg} and the liquid momentum flux parameter C_{vf}.

really close to one. For counter-current flow, the right hand side of Eq. (26) becomes always positive for positive gas velocity. Then Eqs. (29) and (30) determine the stable boundary.

4. Stability of a simplified flow configuration

As the flow condition changes, the two-phase flow adjusts its structure according to the conservation laws presented by the two-fluid model. The changes in morphology can be represented by the changes in velocity and void fraction profiles. As the momentum flux parameters represent those changes in the one-dimensional two-fluid model, it is interesting to investigate the role of momentum flux parameters. In the above section it is claimed that the momentum flux parameters determine the stability of the two-phase flow. So, it is possible that the governing differential equation for the two-fluid model can change type similar to that of compressible flow, transonic flow or shock, or it does not change type, if momentum flux parameters vary in such a way that the two-fluid model becomes always stable. Here, we look at the changes in momentum flux parameters and stability of a two-fluid model in simplified two-phase flow configurations.

4.1. Momentum flux parameters

The experimental data for the void fraction profile and velocity profiles can be approximated by a power-law profile. We will look into the stability of these flow profiles by calculating the momentum flux parameters and compare it with the stability criteria determined in Section 3. The void fraction profile and velocity profile in bubbly and slug flow can be approximated by power-law profile [2,12] as follows

$$\alpha = \alpha_w + \Delta(1 - r^n) \tag{33}$$

$$v_g = v_{wg} + v_{og}(1 - r^m) \tag{34}$$

$$v_f = v_{wf} + v_{of}(1 - r^q) \tag{35}$$

where $\Delta = (\alpha_o - \alpha_w)$. α_o is void fraction at the center, α_w is void fraction at the wall, and r is the non-dimensional radial position. v_{wg} is gas velocity very near wall, v_{og} is gas relative velocity at the center, v_{wf} is liquid velocity very near the wall, v_{of} is liquid relative velocity at the center. Average void fraction and velocity are determined as

$$\langle \alpha \rangle = \alpha_w + \Delta n/(n+2) \tag{36}$$

$$\langle\langle v_g \rangle\rangle = \langle \alpha v_g \rangle / \langle \alpha \rangle \tag{37}$$

$$\langle\langle v_f \rangle\rangle = \langle v_f - \alpha v_f \rangle / \langle 1 - \alpha \rangle \tag{38}$$

Then, the momentum flux distribution parameter for gas is defined as

$$C_{vg} = \langle \alpha v_g^2 \rangle / \langle \alpha \rangle \langle\langle v_g \rangle\rangle^2 = \langle \alpha \rangle \langle \alpha v_g^2 \rangle / \langle \alpha v_g \rangle^2 \tag{39}$$

Assuming that the velocities of gas and liquid at the wall are negligibly small.

$$\begin{aligned} \langle \alpha v_g \rangle &= \langle \alpha \rangle \langle v_g \rangle \\ &\quad + \Delta v_{go} n/(n+2) m/(m+2)\, 2/(n+m+2) \end{aligned} \tag{40}$$

$$\begin{aligned} \langle \alpha v_g^2 \rangle &= \langle \alpha \rangle \langle v_g \rangle^2 + [v_{og} m/(m+2)]^2/(m+1)\langle \alpha \rangle \\ &\quad + \Delta v_{og}^2 n/(n+2) m/(m+2) m/(m+1) 2 \\ &\quad /(2m+n+2)[1 + (2m+2)/(m+n+2)] \end{aligned} \tag{41}$$

With similar argument the momentum flux parameter for liquid flow becomes,

$$C_{vf} = \langle \alpha_f v_f^2 \rangle / \langle \alpha_f \rangle \langle\langle v_f \rangle\rangle^2 = \langle \alpha_f \rangle \langle \alpha_f v_f^2 \rangle / \langle \alpha_f v_f \rangle^2 \tag{42}$$

$$\begin{aligned} \langle \alpha_f v_f \rangle &= (1 - \langle \alpha \rangle)\langle v_f \rangle \\ &\quad - \Delta v_{fo} q/(q+2) n/(n+2) 2/(n+q+2) \end{aligned} \tag{43}$$

$$\begin{aligned} \langle \alpha_f v_f^2 \rangle &= \langle 1 - \alpha \rangle \langle v_f \rangle^2 + [v_{of} q/(q+2)]^2/(q+1)\langle 1 - \alpha \rangle \\ &\quad - \Delta v_{of}^2 n/(n+2) q/(q+2) q/(q+1) 2 \\ &\quad /(2q+n+2)[1 + (2q+2)/(q+n+2)] \end{aligned} \tag{44}$$

The preceeding equations show that momentum flux parameters are functions of n, m, q, α_o, α_w, v_{og}, v_{of}. They change their values according to the various driving forces, which appear on the right hand side of momentum equations. It is a plausible assumption that the momentum flux parameters change in such a way that the two-fluid model becomes always stable.

4.2. Volumetric distribution parameter and average slip ratio

There are many experimental data for gas, liquid velocities and void fraction profiles [13–17]. However, the data are not complete enough to determine all of the parameters for power-law profile. Therefore, we selected the simplified flow configuration to investigate the physical significance of the above mentioned stability criteria.

In a dispersed bubbly flow, it can be assumed that the local gas and liquid velocities are the same, when

relative velocity is negligibly small. Then q is equal to m. By using this simplified flow configuration and existing correlation for volumetric distribution parameter C_o, we can calculate momentum flux parameters. Then, we can compare it with the stability criteria. According to Ishii [12] the effect of void profile over a cross-section is typically presented by the volumetric distribution parameter defined as

$$C_o = \langle \alpha j \rangle / \langle \alpha \rangle \langle j \rangle \tag{45}$$

where j is volumetric flux. When the void fraction is less than 0.7, a lot of data for pipe flow are correlated [12] as

$$C_o = (1.2 - 0.2\sqrt{(\rho_g/\rho_f)})(1 - e^{-18\langle \alpha \rangle}) \tag{46}$$

which is a function of average void fraction and density ratio.

Assuming that liquid and gas velocities at the wall are very close to zero, the volumetric distribution parameter is determined as

$$C_o = 1 - 2/(m + n + 2)(\alpha_w/\langle \alpha \rangle - 1) \tag{47}$$

and by definition slip ratio is

$$S = \langle\langle v_g \rangle\rangle / \langle\langle v_f \rangle\rangle = (1 - \langle \alpha \rangle)C_o/(1 - C_o\langle \alpha \rangle) \tag{48}$$

Since distribution parameter C_o is a function of an average gas void fraction and the density ratio, if the velocity profile is known the power n of the void fraction profile and slip ratio are uniquely determined by C_o and the average void fraction at a given density ratio. As two parameters slip-ratio S and modified density ratio R determine the stability criteria derived in Section 3, we can compare the momentum flux parameters determined by this procedure and those allowed by stability criteria.

4.3. Center-peaked void fraction

Experimental researches [13–17] indicate that the void fraction has a power law profile with center-peak shape when the void fraction is between 0.2 and 0.7 for adiabatic air–water flow. To approximate this profile, let us assume wall void fraction is very close to zero. Then the momentum flux parameters are determined as

$$C_{vf} - 1 = (m + 2)/(m + 1)[1 + I(m, C_o)]/C_o^2 \tag{49}$$

$$C_{vg} - 1 = (1 - \langle \alpha \rangle)(m + 2)/(m + 1)[1 - \langle \alpha \rangle - \langle \alpha \rangle I(m, C_o)]/(1 - \langle \alpha \rangle C_o)^2 \tag{50}$$

where $I(m, C_o) = 2(C_o - 1)[1 + (m + 1)(C_o - 1)]/[m(C_o - 1) + 2]$.

By using the assumption that the liquid and gas profiles are close to a single phase turbulent profile, we can select m as 7 or 8. Then the power for the void fraction profile is determined by equating Eqs. (46) and (47). Here, we assumed density ratio 1000 as a typical number for air–water flow. It is found that as void fraction is increased, the void fraction profile becomes center peaked and centerline void fraction increases. We can find an appropriate void fraction profile with average void fraction between 0.2 and 0.4. However, as the void faction is less than 0.2, the exponent of void profile becomes negative. As the void fraction becomes bigger than 0.4, the centerline void fraction becomes bigger than one, which is physically unrealistic. This suggests that the liquid velocity profile might be quite different from the single-phase turbulent profile. van der Welle [15] found in his experiment that the exponent of power law profile for liquid changes as void fraction changes. He proposed an exponent of power profile, which decreases as void fraction decreases. Though his power law profile is slightly different from ours, we employed the same exponent for convenience

$$m = 10(1 - \langle \alpha \rangle) \tag{51}$$

As the void fraction increases, it becomes a parabolic profile. By employing this profile, we can obtain the reasonable void fraction profile which satisfies the volumetric distribution parameter correlation (46), when the average void fraction is between 0.2 and 0.7.

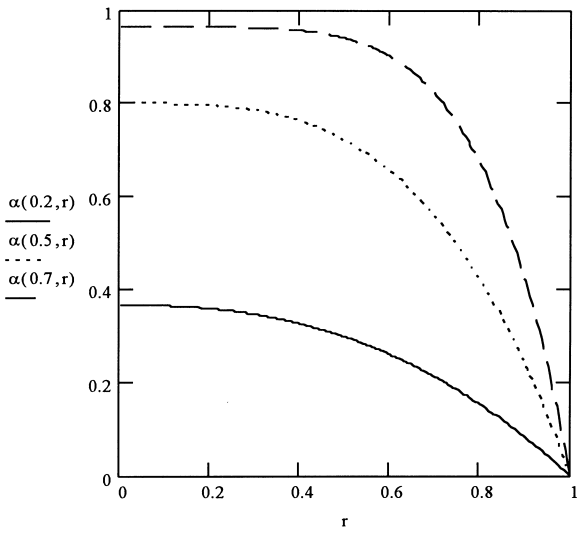

Fig. 3. Void fraction profile at average void fraction of 0.2, 0.5, and 0.7.

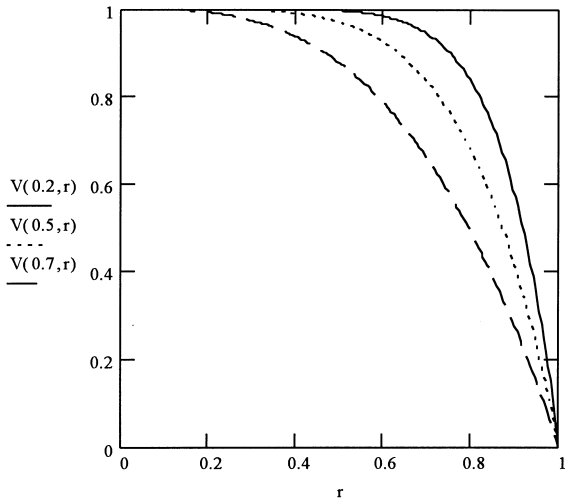

Fig. 4. Velocity profile at average void fraction of 0.2, 0.5, and 0.7.

Figs. 3 and 4 show the void fraction profile and the velocity profile respectively as the average void fraction changes. The trends of the void fraction profile are in good agreement with experimental observations. From Eqs. (49) and (50), the momentum flux parameter is determined as a function of void fraction and distribution parameter C_o. Fig. 5 shows calculated momentum flux parameters for gas and liquid as a function of average void fraction.

At a given density ratio, we can calculate the stability boundary defined in Section 3 which is a function

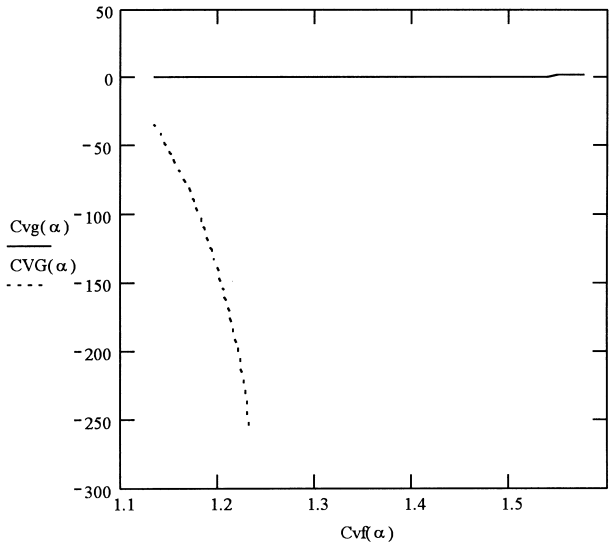

Fig. 6. Comparison of stability boundary CVG and calculated C_{vg} as a function of C_{vf}.

of slip-ratio and modified density ratio R depending on void fraction. In Fig. 6, we compared the calculated momentum flux parameters with the stability criteria defined by Eq. (31) in Section 3. Surprisingly, it is shown that the proposed power law profile is stable and located well above the stability boundary. As the slip ratio is bigger than 1, another stability boundary defined by Eq. (28) is also shown in Fig. 7. It is shown that as the void fraction becomes bigger than 0.45, the

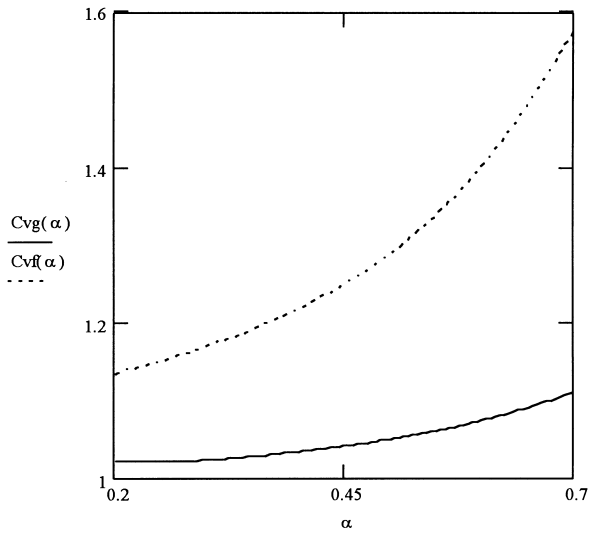

Fig. 5. Liquid momentum flux parameter C_{vf} and gas momentum flux parameter C_{vg} as a function of void fraction α.

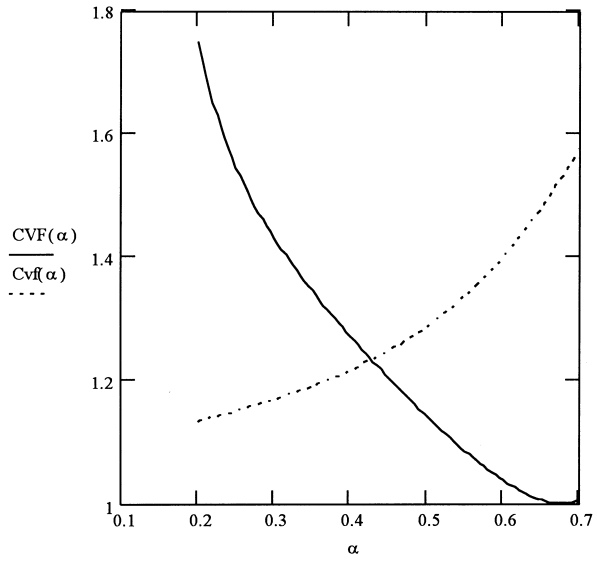

Fig. 7. Comparison of stability boundary CVF and calculated C_{vf} as a function of void fraction α.

calculated liquid momentum flux parameter is bigger than the stability boundary.

4.4. Wall-peaked void fraction profile

Wall-peaked void fraction profile is observed experimentally at low void fraction. Serizawa et al. [13] measured water velocity, air velocity, and void fraction profile for the air–water flow in vertical pipe. He indicated that for the bubbly flow the bubbles are packed near the wall. As the flow changes to slug flow the bubbles are concentrated near the center. Liu and Bankoff [16,17] did similar measurements. They found that void fraction profiles show a distinct peak near the wall. It is clear that the void profile at subcooled boiling shows a wall-peaked void fraction.

In Section 4.3 we indicated that we can not obtain an appropriate power law void fraction profile with the wall void fraction equal to zero, when the void fraction is less than 0.2. Therefore, it is necessary to change our assumption that the wall void fraction is zero. We can maintain the assumption that liquid velocity profile is close to single-phase turbulent profile when gas void fraction is small. Since the profile should be continuous at void fraction of 0.2, we assumed that the velocity profile is the same as that at a void fraction of 0.2 and the exponent of void profile is inversely proportional to the average void fraction. Then the Eqs. (46) and (47) determine the wall void fraction as a function of average void fraction and the density ratio. Fig. 8 shows the gas void fraction profiles as the average void fraction changes. It is shown that at a low average void fraction the void profile becomes wall peaked. This is in good agreement with experimental observations [13,16,17].

The stability of this profile can be examined by calculating the momentum flux parameters. The momentum flux parameters are determined only as a function of average void fraction from Eqs. (40)–(43). Fig. 9 shows calculated momentum flux parameters for gas and liquid. It is shown that the gas momentum flux parameter decreases and liquid momentum flux parameter decreases as the void fraction increases. Though, we can obtain a reasonable void fraction profile at a very low void fraction, the momentum flux parameter shows singular behavior at a very low void fraction. In Fig. 10, we compared the calculated momentum flux parameters with the stability criteria defined in Section 3. It is shown that the proposed power law profile is stable and located well above the stability criteria.

4.5. Effect of density ratio

As the volumetric distribution parameter correlation is valid in a wide range of density ratios, we tested another simplified flow configuration with a different density ratio. For simplicity, we considered the case with a density ratio of 100 and an average void fraction between 0.2 and 0.7. We used van der Welle's [15] velocity profile for convenience. Then we can determine void fraction profiles and momentum flux parameters. In Figs. 11 and 12, the comparison with the curve of calculated momentum flux parameters and the curve of stability boundary is shown. It can be easily seen that the flow is stable.

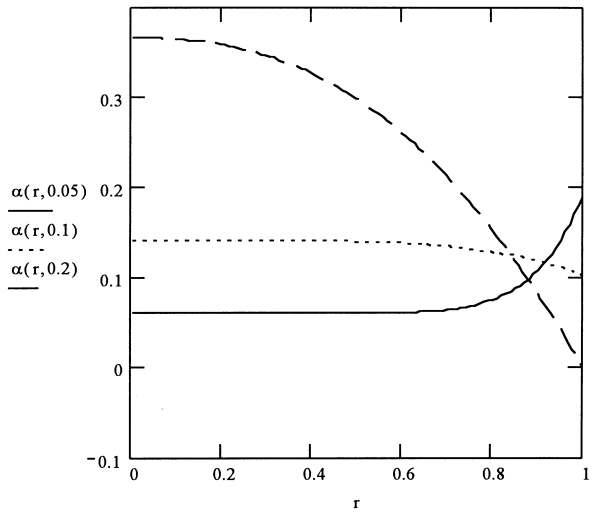

Fig. 8. Void fraction profile at average void fraction of 0.05, 0.1 and 0.2.

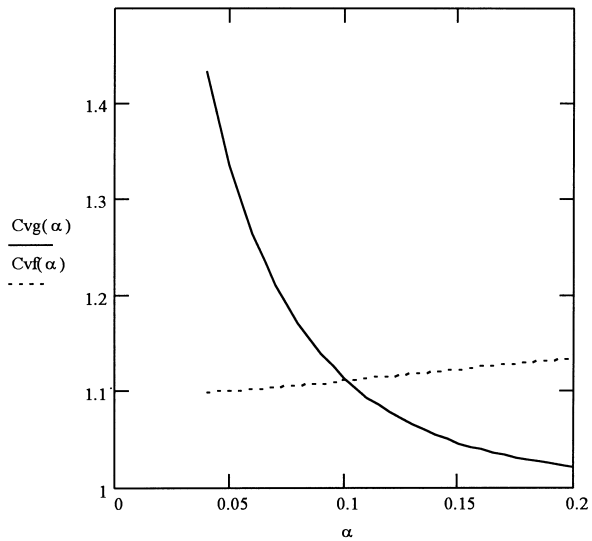

Fig. 9. Liquid momentum flux parameter and gas momentum flux parameter as a function of void fraction α.

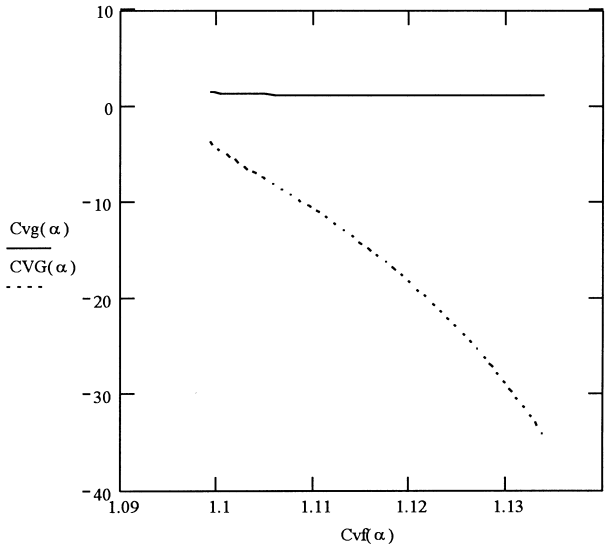

Fig. 10. Comparison of stability boundary CVG and calculated C_{vg} as a function of C_{vf}.

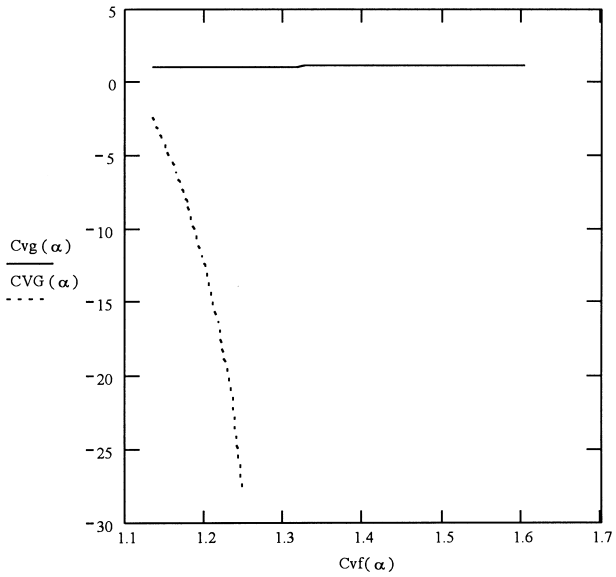

Fig. 11. Comparison of stability boundary CVG and calculated C_{vg} as a function of C_{vf}.

5. Stability of incompressible one-dimensional two-fluid model

The stability of the governing differential equations for the incompressible one-dimensional two-fluid model is described in terms of momentum flux parameters. It is shown that the two-fluid model is stable with certain restrictions on momentum flux parameters. To investigate the physical significance of stability criteria, a simplified two-phase flow configuration of bubbly flow with negligible local slip is considered. By using an existing correlation for the volumetric distribution parameter and experimental velocity profiles, void fraction profiles are obtained at a void fraction of 0.05–0.7. Their trends are in good agreement with experimental observations. The calcu-

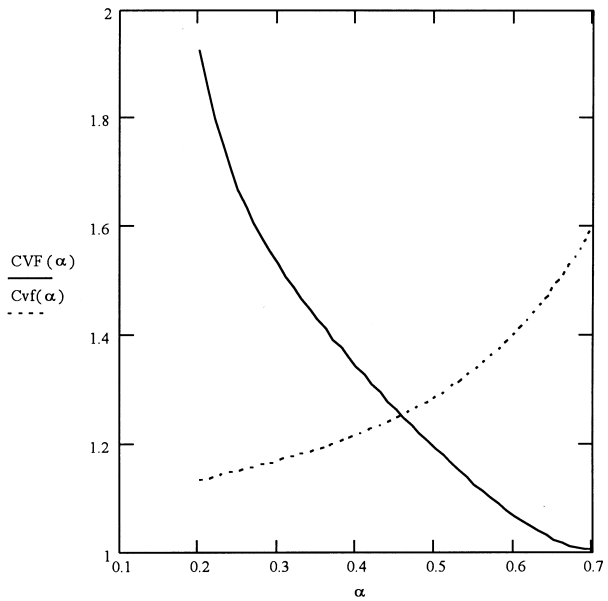

Fig. 12. Comparison of stability boundary CVF and calculated C_{vf} as a function of void fraction α.

lated momentum flux parameters are found to be located well above the stability boundary. As the volumetric distribution parameter is valid in a wide range of density ratios, we looked at the applicability of proposed argument at a different density ratio. The results were satisfactory. It is suggested that the two-phase flow structure change its shape in such a way that the system of governing differential equations remains hyperbolic. As the momentum flux parameter represents the flow structure of a two phase flow, such as, velocity and void fraction variations over a flow area, the stability criteria defined by momentum flux parameters have physical significance.

The majority of the computer codes for nuclear reactor safety, typically represented by RELAP5/MOD3 [3], are using one-dimensional two-fluid models without momentum flux parameters. This kind of one-dimensional two-fluid model is intrinsically unstable as indicated by Gidaspow [4]. The present analysis suggests use of proper momentum flux parameters, which will make the one-dimensional two-fluid model always hyperbolic. As the momentum flux parameters reflect the two-phase flow structure, this proposition is quite natural and reflects physical phenomena. It also is noted that as the momentum flux parameters are close to one, the use of these parameters will not change the previous analysis results drastically. Though they have some restrictions, the momentum flux parameters determined in this paper can be used for a pilot computer code practically.

6. Conclusion

By employing momentum flux parameter, the present paper demonstrated that incompressible one-dimensional two-fluid model is stable with certain restrictions on momentum flux parameters for gas and liquid. A simplified two-phase flow configuration is considered. By using existing correlation and experimental results, the tested flow configuration is found to be in the stable region, when compared with stability criteria described by momentum flux parameters. These analyses results suggest that the one-dimensional two-fluid model should be used with momentum flux parameters. It is beneficial because it reflects flow structure and it helps to stabilize the governing differential equations.

Acknowledgements

This research was supported by the Korean Ministry of Science and Technology.

References

[1] M. Ishii, Thermo-fluid Dynamic Theory of Two-phase Flow, Eyrolles, Paris, 1975.
[2] M. Ishii, K. Mishima, Two-fluid model and hydrodynamic constitutive relations, Nuclear Engineering and Design (1984) 107–126.
[3] Ransom et al., RELAP5/MOD3 Code manual; NUREG/CR-5535, Idaho National Engineering Laboratory, 1995.
[4] D. Gidaspow, Modeling of two phase flow. In: Proceedings of the Fifth International Heat Transfer Conference, 1974, VII. p. 163.
[5] J.H. Stuhmiller, The influence of interfacial pressure forces on the character of two-phase flow model equations, Int. J. Multiphase Flow 3 (1977) 551–560.
[6] A.V. Jones, A. Prosperetti, On the stability of first-order differential models for two-phase flow prediction, Int. J. Multiphase Flow 11 (2) (1985) 133–148.
[7] R.T. Lahey, et al., The effect of virtual mass on the numerical stability of accelerating two-phase flow, Int. J. Multiphase Flow 6 (1980) 281–294.
[8] N. Brauner, D.M. Maron, Stability analysis of stratified liquid–liquid flow, Int. J. Multiphase Flow 18 (1) (1992) 103–121.
[9] S. Kalkach-Navarro, R.T. Lahey, D.A. Drew, Analysis of the bubbly/slug flow regime transition, Nuclear Engineering and Design 151 (1994) 15–39.
[10] C.K. Sung, M.H. Chun, Onset of slugging criterion based on singular points and stability analyses of transient one dimensional two-phase flow equations of two-fluid model, J. Korean Nuclear Society 28 (3) (1996) 299–310.
[11] R.W. Lyczkowski, et al., Characteristic and stability analyses of transient one-dimensional two-phase flow equations and their finite difference approximations, Nuclear Science and Engineering 66 (1978) 378–396.
[12] M. Ishii, One dimensional drift-flux model and constitutive equations for relative motion between phases in various two-phase flow regimes, ANL-77-47, Argonne National Laboratory, 1977.
[13] A. Serizawa, I. Kataoka, I. Michiyoshi, Turbulence structure of air–water bubbly flow — II. Local properties, Int. J. Multiphase Flow 2 (1975) 235–246.
[14] R.A. Herringe, M.R. Davis, Structural development of gas–liquid mixture flows, J. Fluid Mech. 73 (1) (1976) 97–123.
[15] R. van der Welle, Void fraction, bubble velocity and bubble size in two-phase flow, Int. J. Multiphase Flow 11 (3) (1985) 317–345.
[16] T.J. Liu, S.G. Bankoff, Structure of air–water bubbly flow in a vertical pipe — I. Liquid mean velocity and turbulence measurements, Int. J. Heat Mass Transfer 36 (4) (1993) 1049–1060.
[17] T.J. Liu, S.G. Bankoff, Structure of air–water bubbly flow in a vertical pipe — II. Void fraction, bubble velocity and bubble size distribution, Int. J. Heat Mass Transfer 36 (4) (1993) 1049–1060.